

TR/09/82

September 1982

The determination of the poles of the mapping function and their use in numerical conformal mapping.

N. Papamichael, M.K. Warby and D.M. Hough\*

\* Division of Mathematics, Polytechnic of the South Bank, Wandsworth Road, London SW8 2JZ.



## ABSTRACT

Let  $f$  be the function which maps conformally a simply-connected domain  $\Omega$  onto the unit disc. This paper is concerned with the problem of determining the dominant poles of  $f$  in  $\text{comp}1(\Omega \cap \partial\Omega)$ , and of using this information in order to obtain accurate numerical approximations to  $f$  by means of the Bergman kernel method.



1. Introduction

Let  $\Omega$  be a bounded simply-connected domain with boundary  $\partial\Omega$  in the complex  $z$ -plane and assume, without loss of generality, that the origin  $0$  lies in  $\Omega$ . Also, let

$$w = f(z), \quad (1.1)$$

be the function which maps conformally  $\Omega$  onto the unit disc

$$D = \{w : |w| < 1\}, \quad (1.2)$$

so that  $f(0) = 0$  and  $f'(0) > 0$ .

This paper is concerned with the problem of determining the dominant poles of the mapping function  $f$  in  $\text{comp}1(\Omega \cup \partial\Omega)$ , i.e. the poles of the analytic extension of  $f$  which lie close to the boundary  $\partial\Omega$ . Our motivation for considering this problem emerges from the study of certain expansion methods for numerical conformal mapping. These methods lead to approximations to  $f$  of the form

$$f_n(z) = \sum_{j=1}^n a_j u_j(z), \quad (1.3)$$

and the significance of knowing the poles of  $f$  concerns the choice of the set of basis functions  $\{u_j(z)\}$ . More specifically, the significance of the work of the present paper emerges from the observation that the computational efficiency of the numerical mapping techniques improves considerably when the basis set includes terms that reflect the singular behaviour of the dominant poles of  $f$ ; see Levin et al [5], Papamichael and Kokkinos [7] and Ellacott [1].

The dominant poles of  $f$  can be determined easily by means of the Schwarz reflection principle in the case where the boundary  $\partial\Omega$  consists of straight line segments and circular arcs. If this is so, then  $f$

has simple poles at the finite inverse (symmetric) points of the origin with respect to the straight line segments and the circular arcs; see e.g. Nehari [6, p. 184] and Henrici [4, p.389]. If  $\partial\Omega$  is more general than a curve consisting of straight lines and circular arcs, then the situation regarding the location and nature of the poles of  $f$  is much more involved. However, in many cases, it is possible to determine the dominant poles of  $f$  by using a method based on a generalization of the reflection principle. This generalization concerns the continuation of the mapping function across analytic arcs, and is often referred to as the symmetry principle of analytic arcs; see e.g. Henrici [4, p.391] and Sansone and Gerresten [9, p.102].

The details of the presentation are as follows. In Section 2 we explain how the generalized symmetry principle can be used to determine the poles of  $f$  corresponding to an analytic arc  $\Gamma$ . In Section 3 we present three specific applications, by considering in detail the three cases where  $\Gamma$  is respectively an arc of an ellipse, a parabola and a hyperbola. Finally, in Section 4 we present several examples illustrating the significance of the work of the present paper, in connection with numerical conformal mapping techniques. In each of these examples the approximation to  $f$  is computed by using an expansion method based on the theory of the Bergman kernel function of  $\Omega$ . This method has been studied recently in [5] and [7].

## 2. The poles of the mapping function with respect to an analytic arc.

With the notation of Section 1, let  $\Gamma$  be an analytic arc of  $\partial\Omega$  with parametric equation

3.

$$z = p(s), \quad s_1 < s < s_2$$

i.e.

$$\Gamma = \{z : z = p(s), \quad s_1 < s < s_2\} \quad (2.1)$$

Also, let  $G^*$  be a simply-connected domain in the complex  $\zeta$ -plane,  $\zeta = s + it$ , such that the following two conditions hold.

C 2.1. The function

$$z = P(\zeta), \quad (2.2)$$

is one-one analytic in  $G^*$ .

C 2.2. The domain  $G^*$  has a symmetric partition with respect to the straight line segment

$$L = \{\zeta : \zeta = s + it, \quad s_1 < s < s_2, \quad t = 0\}, \quad (2.3)$$

so that

$$G^* = G_1 \cup L \cup G_2, \quad (2.4)$$

where the image  $\Omega_1$  of  $G_1$ , under the transformation (2.2), is contained within  $\Omega$ , i.e.  $\Omega_1 \subseteq \Omega$ . Clearly, the symmetric subdomains  $G_1$  and  $G_2$  of  $G^*$  may be given either by

$$G_1 = \{\zeta : \zeta \in G^* \text{ and } t > 0\} \text{ and } G_2 = \{\zeta : \zeta \in G^* \text{ and } t < 0\}, \quad (2.5)$$

or by

$$G_1 = \{\zeta : \zeta \in G^* \text{ and } t < 0\} \text{ and } G_2 = \{\zeta : \zeta \in G^* \text{ and } t > 0\}. \quad (2.6)$$

If the conditions C2.1 and C2.2 hold then the function (2.2) maps conformally  $G^*$  onto a domain

$$\Omega^* = \Omega_1 \cup \Gamma \cup \Omega_2, \quad (2.7)$$

so that the straight line  $L$  and the domains  $G_j$ ;  $j = 1, 2$ , are mapped respectively onto the arc  $\Gamma$  and the domains  $\Omega_j$ ;  $j = 1, 2$ . Thus the function

$$h(\zeta) = f(p(\zeta)), \quad (2.8)$$

where  $f$  is the mapping function (1.1), is one-one analytic in  $G_1 \cup L$  and

$$w = h(\zeta), \quad (2.9)$$

maps the straight line  $L$  onto an arc of the unit circle. Therefore, by the reflection principle, the function

$$H(\zeta) = \begin{cases} h(\zeta), & \zeta \in G_1 \cup L, \\ 1/\overline{h(\bar{\zeta})}, & \zeta \in G_2, \end{cases} \quad (2.10)$$

is meromorphic in  $G_2$  and defines the analytic continuation of  $h$ , across  $L$ , into  $G_2$ .

Let  $q$  be the inverse function of  $p$ , i.e.

$$q = p^{[-1]}, \quad (2.11)$$

and let

$$a(z) = p(\overline{q(z)}). \quad (2.12)$$

Then, in view of (2.8) and (2.10), the function

$$F(z) = H(q(z)) = \begin{cases} f(z), & z \in \Omega_1 \cup \Gamma, \\ 1/\overline{f(a(z))}, & z \in \Omega_2, \end{cases} \quad (2.13)$$

is analytic in  $\Omega_1$ , meromorphic in  $\Omega_2$  and defines the analytic continuation of the mapping function  $f$  across  $\Gamma$  into  $\Omega_2$ . This analytic extension of  $f$  is a particular case of the symmetry principle of analytic arcs, and the points  $z$  and  $a(z)$  are called symmetric points with respect to the arc  $\Gamma$ . As it is shown in [9, p.103], symmetric points are independent of the parametrization of  $\Gamma$ .



The above analysis leads to the following results regarding the location and nature of poles of the function  $F$ .

R2.1. If  $0 \in \Omega_1$  then the equation

$$p(\zeta) = 0, \quad (2.14)$$

has exactly one root  $\zeta_0$  in  $G_1$ . Hence, it follows easily from (2.8), (2.10), and (2.13), that the function  $F$  has a simple pole at the point  $z_0 \in \Omega_2$ , where

$$\begin{aligned} z_0 &= p(\bar{\zeta}_0) \\ &= a(0), \end{aligned} \quad (2.15)$$

is the inverse point of the origin with respect to  $\Gamma$ .

R2.2. If  $0 \in \partial\Omega_1/\Gamma$  then the equation (2.14) has at least one root  $\zeta_0 \in \partial G/L$  and we may assume, without much loss of generality, that  $p$  is analytic at  $\zeta_0$  and  $\bar{\zeta}_0$ . However,  $p$  is not necessarily one-one in the neighbourhood of these points. For this reason, we let

$$p(\zeta) = (\zeta - \zeta_0)^m p_1(\zeta), \quad p_1(\zeta) \neq 0, \quad m \geq 1, \quad (2.16)$$

$$p(\zeta) - p(\bar{\zeta}_0) = (\zeta - \bar{\zeta}_0)^n p_2(\zeta), \quad p_2(\bar{\zeta}_0) \neq 0, \quad n \geq 1, \quad (2.17)$$

and, in order to determine the behaviour of  $F$  at the point

$$z_0 = p(\bar{\zeta}_0) \in \partial\Omega_2/\Gamma, \quad (2.18)$$

we proceed as follows.

The mapping function  $f$  is of the form

$$f(z) = z f_1(z), \quad (2.19)$$

where  $f_1(0) \neq 0$ . Therefore, from (2.13), when  $z \in \Omega_2$ , the function

$$G(z) = 1/F(z), \quad (2.20)$$

has the form

6.

$$G(z) = \overline{a(z)} G_1(z) , \quad (2.21)$$

where  $G_1$  is analytic at  $z_0$  and  $G_1(z_0) \neq 0$ . Also, from (2.12) and (2.16)

$$\overline{a(z)} = (q(z) - q(z_0))^m a_1(z) , \quad (2.22)$$

and, from (2.17),

$$q(z) - q(z_0) = (z - z_0)^{1/n} q_1(z) , \quad (2.23)$$

where  $a_1$  and  $q_1$  are analytic and non-zero at  $z_0$ . Hence, by combining (2.22) and (2.23),

$$\overline{a(z)} = (z - z_0)^{m/n} (q_1(z))^m a_1(z) , \quad (2.24)$$

and therefore, from (2.21),

$$G(z) = (z - z_0)^{m/n} G_2(z) , \quad (2.25)$$

where  $G_2$  is analytic and non-zero at  $z_0$ . Thus, the nature of the singularity of  $F$  at  $z_0$  depends on the values of the integers  $m$  and  $n$  in (2.16) and (2.17). The following three cases occur frequently in applications.

- (a)  $m = n = 1$ . In this case  $F$  has a simple pole at  $z_0$ .
- (b)  $m = 2, n = 1$ . In this case  $F$  has a double pole at  $z_0$ .
- (c)  $m = 1, n = 2$ . In this case  $F$  has a singularity of the form  $(z - z_0)^{-\frac{1}{2}}$ .

R.2.3. If  $0 \notin \Omega_1 \cup (\partial\Omega_1/\Gamma)$  then  $F$  has no poles in  $\Omega_2 \cup (\partial\Omega_1/\Gamma)$ .

Naturally, if  $\Gamma$  is a straight line or a circular arc then the above procedure for determining the poles of  $F$  leads to the well-known results predicted by the reflection principle. That is, if  $0 \in \Omega_1 \cup (\partial\Omega_1/\Gamma)$  then  $F$  has a simple pole at the point  $p(\bar{\zeta}_0) \in \Omega_2 \cup (\partial\Omega_2/\Gamma)$ ,

where the symmetric point  $p(\bar{\zeta}_0)$  coincides with the mirror image of 0 with respect to the straight line or with the geometric inverse of 0 with respect to the circular arc.

In what follows we refer to a singularity of  $F$ , of the type described in R2.1 and R2.2, as "a pole of the mapping function  $f$  with respect to the arc  $\Gamma$ ".

### 3. Particular cases

In this section we illustrate the application of the technique of Section 2 by considering in detail the three cases where  $\Gamma$  is respectively an arc of an ellipse, a parabola and a hyperbola. Naturally, in each of these cases, the poles of  $f$  can also be determined by arguments based on the use of the known exact conformal maps of an ellipse, a parabola and a hyperbola. The reason for preferring the use of the technique of Section 2 is that its application is not restricted to arcs of curves whose exact conformal maps are known.

#### 3.1. Elliptical arc $\Gamma$ .

Let  $\Gamma$  be an arc of the ellipse

$$E: (x-x_c)^2/a^2 + (y-y_c)^2/b^2 = 1, \quad a > b,$$

and let the parametric equation of  $\Gamma$  be

$$\begin{aligned} z &= p(s) \\ &= z_c + ae \cos(s - i\eta), \quad s_1 < s < s_2, \end{aligned} \quad (3.1)$$

where  $z_c = x_c + iy_c$ ,  $e = \left(1 - b^2/a^2\right)^{\frac{1}{2}}$ ,  $\cosh \eta = 1/e$  and  $s_2 - s_1 < 2\pi$ .

Then the function

$$z = p(\zeta), \quad \zeta = s + it \quad (3.2)$$

is one-one analytic in the strip

$$\{\zeta : \zeta = s + it, \quad s_1 < s < s_2, \quad -\infty < t < \eta\}$$

and, with the notation of Section 2, we may take as domain  $G^*$  a symmetric subdomain of the rectangle

$$\{\zeta : \zeta = s + it, \quad s_1 < s < s_2, \quad -\eta < t < \eta\}. \quad (3.3)$$

To simplify the presentation we assume that the condition C2.2 holds when  $G^*$  is the whole rectangle (3.3). Then the domain  $\Omega^* = \Omega_1 \cup \Gamma \cup \Omega_2$  can be deduced easily by determining the images under the transformation (3.2) of the four sides of the rectangle (3.3). To illustrate this we assume, that the orientation of  $\Gamma$  with respect to  $\Omega$  is such that  $G_1$  and  $G_2$  are given by (2.5), and in Figures 3.1-3.4 we present four typical domains  $\Omega^*$ . These domains correspond to the four cases where  $s_1=0$  and the parameter  $s_2$  is such that  $0 < s_2 \leq \pi/2, \pi/2 < s_2 \leq \pi, \pi < s_2 \leq 3\pi/2, 3\pi/2 < s_2 < 2\pi$ , respectively.

In each diagram  $\Gamma = \text{arc } \widehat{PQ}$  and the parametric equations of  $\Gamma' = \text{arc } \widehat{P'Q'}$  and  $\gamma = \text{arc } \widehat{Q'R}$  are respectively

$$z = p(s - i\eta), \quad 0 < s < s_2, \quad (3.4)$$

and

$$z = p(s_2 + it), \quad -\eta < t < \eta. \quad (3.5)$$

That is  $\Gamma'$  and  $\gamma$  are respectively arcs of an ellipse  $E'$  and a hyperbola  $H$ , where  $E'$  and  $H$  have common foci with the ellipse  $E$ . Naturally, the hyperbola  $H$  cuts the ellipses  $E$  and  $E'$  orthogonally. We observe that  $\gamma$  is an arc of the right-hand branch of  $H$  if  $\text{coss}_2 > 0$ , and of the left-hand branch if  $\text{coss}_2 < 0$ . We also observe that if  $s_2 = \pi/2, \pi$  or  $3\pi/2$

then the hyperbola  $H$  degenerates into a straight line. More precisely, if  $s_2 = \pi/2$  or  $3\pi/2$  then the point  $R$  coincides with the centre  $C$  of  $E$  and  $\gamma$  becomes a segment of the minor axis of  $E'$ . Similarly, if  $s_2 = \pi$  then the point  $R$  coincides with the focus  $F_2 = (x_c - ae, y)$  and  $\gamma$  becomes a segment of the major axis of  $E'$ .

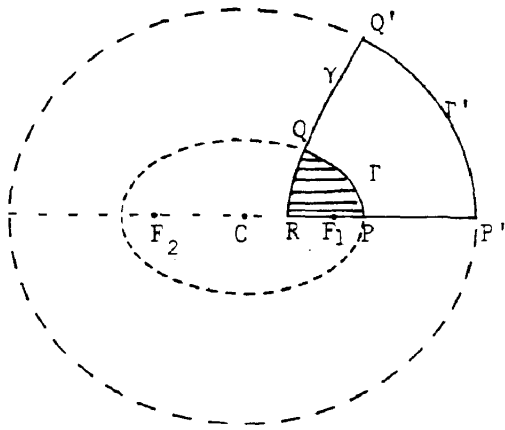


Figure 3.1

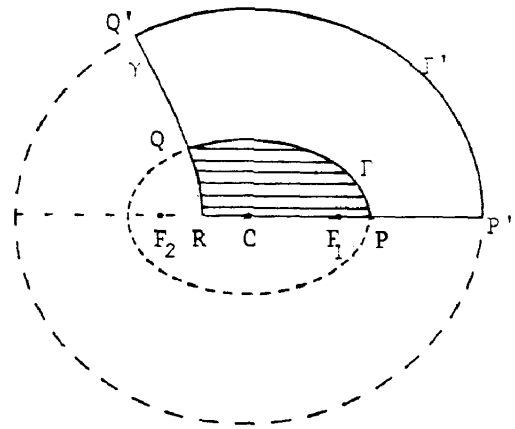


Figure 3.2

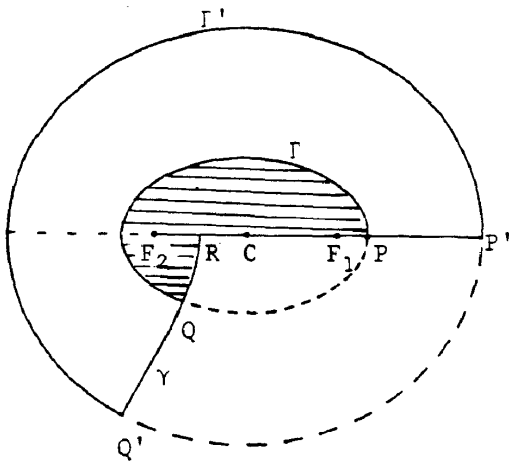


Figure 3.3

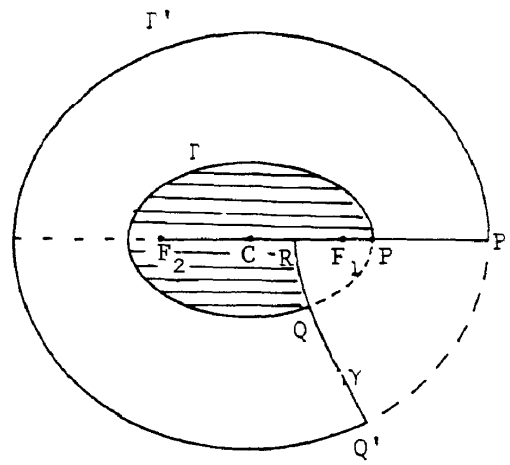


Figure 3.4

In each diagram  $\Omega_1$  is the shaded region, and  $\Omega_2$  is the region bounded by the arcs  $\Gamma$  and  $\Gamma'$  and the subarc  $\widehat{Q'Q}$  of  $\gamma$ . It is important to observe that if  $s_2 > \pi$  then the domain  $\Omega_1$  involves a cut along the straight line joining the focus  $F_2$  to the point  $R$ . This is due to the fact that under the mapping (3.2) the points  $(\pi \pm s) + in$ ,  $s > 0$ , have the common image  $z_c - ae \cos s$ .

The nature of the domain  $\Omega^*$  corresponding to any arc  $\Gamma$  with  $0 \leq s_1 < s_2 < 2\pi$  can be deduced easily from the domains illustrated in Figures 3.1 - 3.4. For example, the domain corresponding to an arc  $\Gamma$  with  $0 < s_1 \leq \pi/2$  and  $\pi < s_2 < 3\pi/2$ , is obtained by deleting the domain of Figure 3.1 from that of Figure 3.3. The domain  $\Omega^*$  corresponding to an arc  $\Gamma$  which includes the two vertices  $z_c \pm a$  of  $E$  can also be deduced from the domains of Figures 3.1 - 3.4. For example, if  $-\pi/2 < s_1 < 0$  and  $\pi < s_2 < 3\pi/2$ , then  $\Omega^*$  is given by the union of the domain of Figure 3.3 with that obtained by reflecting the domain of Figure 3.1 about the major axis.

Corresponding to the general results R2.1 - R2.3 of Section 2, the situation regarding the nature of poles of the mapping function  $f$  with respect to an elliptical arc  $\Gamma$ , orientated so that  $G_1$  and  $G_2$  are given by (2.5), is as follows.

R.3.1.1. If  $0 \in \Omega_1$  then the equation

$$p(\zeta) = 0, \quad (3.6)$$

has exactly one root in  $G_1$  given by

$$\zeta_0 = in + \cos^{-1}(-z_c/ae). \quad (3.7)$$

This means that  $f$  has a simple pole at the point  $z_0 \in \Omega_2$ , where

$$\begin{aligned} z_0 &= p(\bar{\zeta}_0) \\ &= z_c - \left\{ (a^2 + b^2)\bar{z}_c - 2iab(a^2 - b^2 - \bar{z}_c^2)^{\frac{1}{2}} \right\} / (a^2 - b^2). \end{aligned} \quad (3.8)$$

(In (3.8), the branch cut of the square root is taken to be along the positive real axis and  $(-1)^{\frac{1}{2}} = i$ .)

R.3.1.2. If  $0 \in \partial\Omega_1 / \Gamma$  then the situation regarding the poles of  $f$  may be different from that described in R3.1.1 only if  $0$  lies on the major axis of  $E$  between the foci  $F_1$  and  $F_2$ . More precisely, if  $-ae \leq x_c \leq ae$  and  $y_c = 0$  then the following three cases arise,

(a) The region  $\Omega_1$  involves a cut and  $0$  lies on the cut but does not coincide with a focus of  $E$ .

In this case there are two distinct values of  $\cos^{-1}(-x/ae)$  in the interval  $(s_1, s_2)$  and, corresponding to these, the equation (3.6) has two distinct roots on the side  $t = \eta$  of  $G_1$ . For this reason,  $f$  has two simple poles at the two points of  $\Gamma'$  given by

$$z_0 = \left\{ -2b^2x_c \pm 2iab(a^2 - b^2 - x_c^2)^{\frac{1}{2}} \right\} / (a^2 - b^2). \quad (3.9)$$

(b)  $0$  does not lie on a cut of  $\Omega_1$  and does not coincide with a focus of  $E$ .

In this case there is exactly one value of  $\cos^{-1}(-x_c/ae)$  in the interval  $(s_1, s_2)$  and, because of this, (3.6) has one root on the side  $t = \eta$  of  $G_1$ . For this reason,  $f$  has a simple pole at the point  $z_0$  given by (3.9), where the sign in the square brackets is chosen so that  $z$  lies on  $\Gamma'$ .

(c) 0 coincides with one of the foci, i.e.  $x_c = \pm ae, y_c = 0$ .

This case corresponds to the situation described in R2.2(b) of Section 2. That is, the equation (3.6) has a double root at  $\zeta_0 = i\eta$  or  $\zeta_0 = \pi + i\eta$ , depending on whether 0 coincides with  $F_1$  or  $F_2$ . For this reason,  $f$  has a double pole at one of the vertices of the ellipse  $E'$ , i.e. at one of the points

$$z_0 = \pm 2b^2(a^2 - b^2)^{-\frac{1}{2}} \quad (3.10)$$

where the  $\pm$  signs correspond respectively to the cases where 0 is at  $F_1$  and 0 is at  $F_2$ .

R3.1.3. If  $0 \notin \Omega_1 \cup (\partial\Omega/\Gamma)$  then  $f$  has no poles in  $\Omega_2 \cup \Gamma'$ .

If the orientation of the arc  $\Gamma$  with respect to  $\Omega$  is such that  $G_1$  and  $G_2$  are given by (2.6) then, in Figures 3.1 - 3.4, the roles of  $\Omega_1$  and  $\Omega_2$  are reversed, i.e. in each figure the shaded region denotes the domain  $\Omega_2$ . The conclusions contained in R3.1.1 and R3.1.3 remain unaltered but, in this case, R3.1.2 must be replaced by the following.

R3.1.2'. If  $O \in \partial\Omega_1/\Gamma$  then  $f$  has a simple pole at the point  $z_0$  given by (3.8), except when 0 coincides with one of the vertices of the ellipse  $E'$ , i.e. when

$$x_c = \pm (a^2 + b^2)(a^2 - b^2)^{-\frac{1}{2}} \text{ and } y_c = 0 \quad (3.11).$$

The values (3.11) give rise to the situation described in R2.2(c) and, because of this,  $f$  has a singularity of the form

$$(z - z_0)^{-\frac{1}{2}}, \quad (3.12).$$

at one of the foci of  $E$ , i.e. at one of the points

$$z_0 = \pm 2b^2(a^2 - b^2)^{-\frac{1}{2}}. \quad (3.13).$$



### 3.2. Parabolic arc $\Gamma$ .

Let  $\Gamma$  be part of the parabola

$$\pi: (y - y_V)^2 = 4a(x - x_V), \quad a > 0,$$

and let the parametric equation of  $\Gamma$  be

$$\begin{aligned} z &= p(s) \\ &= z_V + a\{(s+i)^2 + 1\}, \quad s_1 < s < s_2, \end{aligned} \quad (3.14)$$

where  $z_V = x_V + iy_V$ . Then, the function

$$z = p(\zeta), \quad \zeta = s + it, \quad (3.15)$$

is one-one analytic in the strip

$$\{\zeta: \zeta = s + it, \quad s_1 < s < s_2, \quad -1 < t < \infty\},$$

and we may take as domain  $G^*$  a symmetric subdomain of the rectangle

$$\{\zeta: \zeta = s + it, \quad s_1 < s < s_2, \quad -1 < t < 1\}. \quad (3.16)$$

Two typical domains  $\Omega^*$  are illustrated in Figures 3.5 and 3.6.

These are obtained under the assumptions that the condition C2.2 holds when  $G^*$  is the whole rectangle (3.16), and the orientation of  $\Gamma$  with respect to  $\Omega$  is such that  $G_1$  and  $G_2$  are given by (2.6). The domains illustrated correspond respectively to the two cases  $0 < s_1 < s_2$  and  $s_1 < 0 < s_2$  with  $|s_1| < |s_2|$ .

In each diagram  $\Gamma = \widehat{\text{arc PQ}}$ , and the parametric equations of  $\Gamma' = \widehat{\text{arc P'Q'}}$ ,  $\gamma_1 = \widehat{\text{arc R}_1\text{P}'}$  and  $\gamma_2 = \widehat{\text{arc R}_2\text{Q}'}$  are respectively

$$z = p(s+i), \quad s_1 < s < s_2, \quad (3.17)$$

$$z = p(s_1+i), \quad -1 < t < 1, \quad (3.18)$$

and

$$z = p(s_2 + it), \quad -1 < t < 1. \quad (3.19)$$

That is  $\Gamma'$ ,  $\gamma_1$  and  $\gamma_2$  are respectively arcs of three parabolas, each having the same focus as  $\Pi$ .

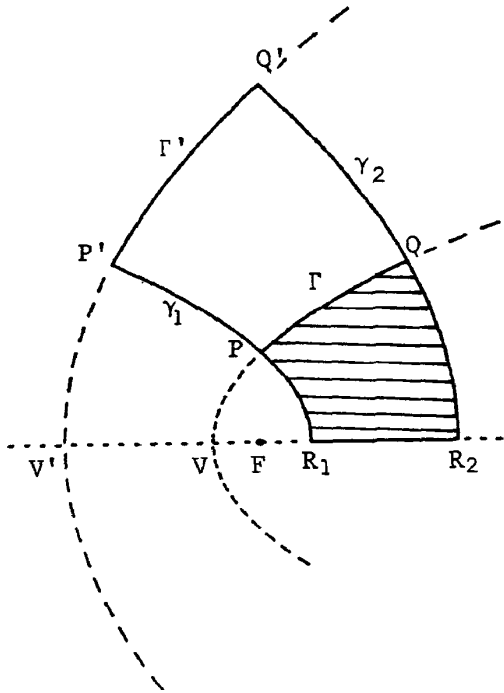


Figure 3.5

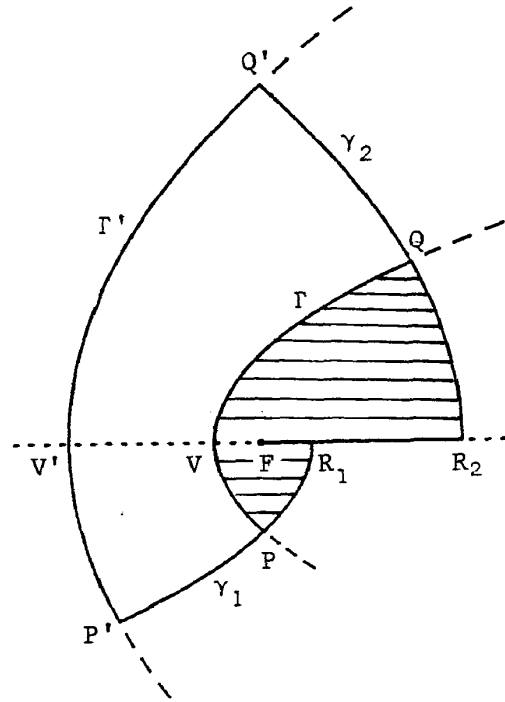


Figure 3.6

In each diagram,  $\Omega_1$  is the shaded region and  $\Omega_2$  is the region bounded by  $\Gamma$ ,  $\Gamma'$  and the subarcs  $\widehat{PP'}$  and  $\widehat{QQ'}$  of  $\gamma_1$  and  $\gamma_2$ . The domain  $\Omega_1$  of Figure 3.6 involves a cut along the straight line joining the point  $R_1$  to the focus  $F$  of  $\Pi$ . This is due to the fact that under the mapping (3.15) the points  $\pm s-i$  have the common image  $z_V + a(s^2 + 1)$ .

If  $G_1$  and  $G_2$  are given by (2.6) then the following results can be established easily, by using arguments similar to those used for establishing the corresponding results R3.1.1 - R3.1.3 of Section 3.1.

R3.2.1. If  $0 \in \Omega_1$  then  $f$  has a simple pole at the point  $z_0 \in \Omega_2$  where

$$z_0 = 2iy_V - 4a \left\{ 1 - i \overline{\left( z_V/a - 1 \right)^{\frac{1}{2}}} \right\} \tag{3.20}$$

(In (3.20) the branch cut of the square root is taken to be along the positive real axis and  $(-1)^{\frac{1}{2}} = i$ .)

R3.2.2. If  $0 \in \partial\Omega_1/\Gamma$  then the situation regarding the poles of  $f$  may be different from that of R3.2.1 only if  $0$  lies on the axis of the parabola, i.e. only if  $x_v \leq -a$  and  $y_v = 0$ . The following three cases arise.

(a) The region  $\Omega_1$  involves a cut and  $0$  lies on the cut but does not coincide with the focus of  $\Pi$ .

In this case  $f$  has two simple poles at the two points of  $\Gamma'$  given by

$$z_0 = -4a \left\{ 1 \pm i \left( -x_v/a - 1 \right)^{\frac{1}{2}} \right\}. \quad (3.21)$$

(b)  $0$  does not lie on a cut of  $\Omega_1$  and does not coincide with the focus of  $\Pi$ .

In this case  $f$  has a simple pole at the point  $z_0$  given by (3.21), where the sign in the square brackets is chosen so that  $z_0$  lies on  $\Gamma'$ .

(c)  $0$  coincides with the focus of  $\Pi$ , i.e.  $x_v = -a, y_v = 0$ .

In this case  $f$  has a double pole at the point

$$z_0 = -4a, \quad (3.22)$$

i.e. at the vertex of the arc  $\Gamma'$ .

R3.2.3. If  $0 \notin \Omega_1 \cup (\partial\Omega_1/\Gamma)$  then  $f$  has no poles in  $\Omega_2 \cup \Gamma'$ .

If the orientation  $\Gamma$  with respect to  $\Omega$  is such that  $G_1$  and  $G_2$  are given by (2.5) then, in Figures 3.5 - 3.6, the roles of  $\Omega_1$  and  $\Omega_2$  are reversed. The only other change concerns the result R3.2.2 which, in this case, must be replaced by the following.

R3.2.2'. If  $0 \in \partial\Omega_1/\Gamma$  then  $f$  has a simple pole at the point  $z_0$  given by (3.20), except when the origin coincides with the vertex of the parabolic arc  $\Gamma'$ , i.e. when

$$x_v = 3a \text{ and } y_v = 0. \quad (3.23)$$

In this case  $f$  has a singularity of the form

$$(z - z_0)^{-\frac{1}{2}} \quad (3.24)$$

at the point

$$z_0 = 4a, \quad (3.25)$$

i.e. at the focus of  $\Pi$ .

### 3.3. Hyperbolic arc $\Gamma$ .

Let  $\Gamma$  be an arc of the right hand branch of the hyperbola

$$H: (x - x_v)^2/a^2 - (y - y_v)^2/b^2 = 1, \quad (3.26)$$

and let the parametric equation of  $\Gamma$  be

$$\begin{aligned} z &= p(s) \\ &= z_v + a \cosh(s + i\eta), \quad s_1 < s < s_2, \end{aligned} \quad (3.27)$$

where  $z_v = x_v + iy_v$ ,  $e = (1 + b^2/a^2)^{1/2}$  and  $\cos\eta = 1/e$ . Then, the function

$$z = p(\zeta), \quad \zeta = s + it, \quad (3.28)$$

is one-one analytic in the strip

$$\{\zeta: \zeta = s + it, s_1 < s < s_2, -\eta < t < \infty\},$$

and we may take as domain  $G^*$  a symmetric subdomain of the rectangle

$$\{\zeta: \zeta = s + it, s_1 < s < s_2, -\eta < t < \eta\}. \quad (3.29)$$

Two typical domains  $\Omega^*$  are illustrated in Figures 3.7 and 3.8. These are obtained under the assumptions that the condition C2,2 holds when  $G^*$  is the whole rectangle (3.29), and the orientation of  $\Gamma$ , with respect to  $\Omega$ , is such that  $G$  and  $G$  are given by (2.5). The domains illustrated correspond respectively to the cases  $0 < s_1 < s_2$  and  $s_1 < 0 < s_2$  with  $|s_1| < |s_2|$ .

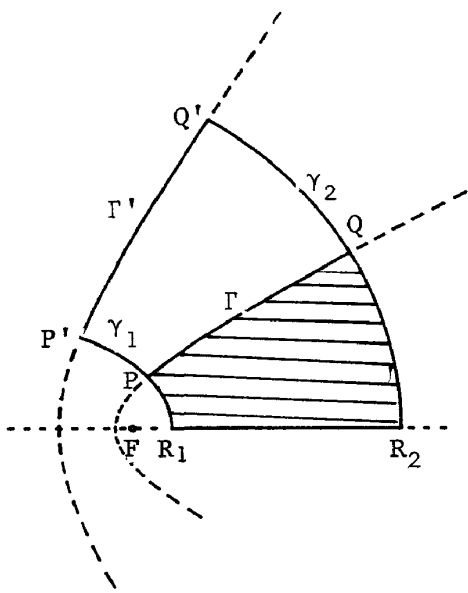


Figure 3.7

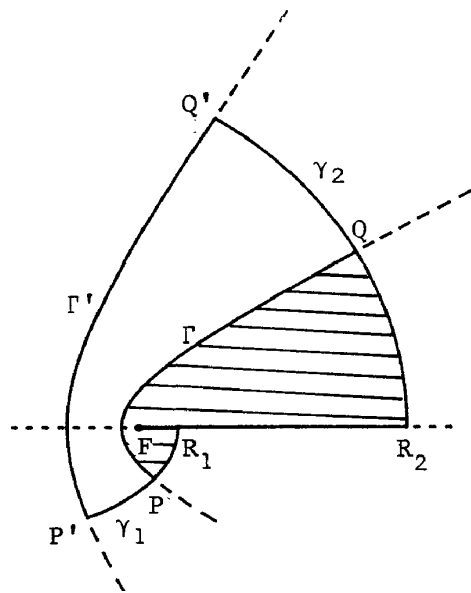


Figure 3.8

In each diagram  $\Gamma = \widehat{PQ}$  and the parametric equations of  $\Gamma' = \widehat{P'Q'}$ ,  $\gamma_1 = \widehat{R_1P'}$  and  $\gamma_2 = \widehat{R_2Q}$  are respectively

$$z = p(s + i\eta), \quad s_1 < s < s_2, \quad (3.30)$$

$$z = p(s_1 + it), \quad -\eta < t < \eta, \quad (3.31)$$

and

$$z = p(s_2 + it), \quad -\eta < t < \eta. \quad (3.32)$$

That is  $\Gamma'$ ,  $\gamma_1$  and  $\gamma_2$  are respectively arcs of a hyperbola  $H'$  and two ellipses  $E_1$  and  $E_2$ , where  $H'$ ,  $E_1$  and  $E_2$  have common foci with  $H$ .

In the diagrams we assumed that  $0 < b < a$  and, for this reason,  $\Gamma'$  is an arc of the right hand branch of  $H'$ . If  $a < b$  then  $\Gamma'$  is an arc of the left hand branch of  $H'$ , and if  $a = b$  then  $\Gamma'$  degenerates into a segment of the straight line  $x = x_v$ . Also, if one of the values  $s_i$ ;  $i = 1, 2$  is zero then respectively one of the arcs  $\gamma_i$ ;  $i = 1, 2$  degenerates into a segment of the axis  $H$ .

In each diagram  $\Omega_1$  is the shaded region and  $\Omega_2$  is the region bounded by  $\Gamma'$  and the subarcs  $\widehat{PP'}$  and  $\widehat{QQ'}$  of  $\gamma_1$  and  $\gamma_2$ . The domain  $\Omega_1$  of Figure 3.8 involves a cut along the straight line joining the point  $R_1$  to the focus  $F$  of  $H$ . This is due to the fact that under the mapping (3.28) the points  $\pm s$  have the common image  $z_v + a \cosh s$ .

If  $G_1$  and  $G_2$  are given by (2.5) then the results regarding the nature of poles of  $f$  are as follows.

R3.3.1. If  $0 \in \Omega_1$  then  $f$  has a simple pole at the point  $z_0 \in \Omega_2$ , where

$$z_0 = z_v - \left\{ (a^2 - b^2)\bar{z}_v + 2iab(\bar{z}_v^2 - a^2 - b^2)^{\frac{1}{2}} \right\} / (a^2 + b^2). \quad (3.33)$$

(In (3.33) the branch cut of the square root is taken to be along the positive real axis and  $(-1)^{\frac{1}{2}} = i$ .)

R3.3.2. If  $0 \in \partial\Omega_1 / \Gamma$  then the situation regarding the poles of  $f$  may be different from that of R3.3.1 only if  $0$  lies on the axis of  $H$ , i.e. only if  $x_v \leq -ae$  and  $y_v = 0$ . The following three cases arise.

(a) The region  $\Omega_1$  involves a cut and  $0$  lies on the cut but does not coincide with the focus  $F$  of  $H$ .

In this case  $f$  has two simple poles at the two points of  $\Gamma'$  given by

$$z_0 = \left\{ 2b^2 x_v \pm 2iab(x_v^2 - a^2 - b^2)^{\frac{1}{2}} \right\} / (a^2 + b^2) . \quad (3.34)$$

(b) 0 does not lie on a cut of  $\Omega_1$  and does not coincide with the focus F of H.

In this case  $f$  has a simple pole at the point  $z_0$  given by (3.34), where the sign in the square brackets is chosen so that  $z_0$  lies on  $\Gamma'$ .

(c) 0 coincides with the focus F of H, i.e.  $x_v = -ae$  and  $y_v = 0$ .

In this case  $f$  has a double pole at the point

$$z_0 = - 2b^2 (a^2 + b^2)^{-\frac{1}{2}} , \quad (3.35)$$

i.e. at a vertex of the hyperbola  $H'$ .

R3.3.3. If  $0 \notin \Omega_1 \cup (\partial\Omega_1 / \Gamma)$  then  $f$  has no poles in  $\Omega_2 \cup \Gamma'$ .

If the orientation of  $\Gamma$  with respect to  $\Omega$  is such that  $G_1$  and  $G_2$  are given by (2.6) then, in Figures 3.7-3.8, the roles of  $\Omega_1$  and  $\Omega_2$  are reversed. The only other change concerns the result R3.3.2 which, in this case, must be replaced by the following.

R.3.3.2' If  $0 \in \partial\Omega_1 / \Gamma$  then  $f$  has a simple pole at the point  $z_0$  given by (3.33), except when the origin coincides with the vertex of the hyperbolic arc  $\Gamma'$ , i.e. when

$$x_v = (b^2 - a^2)(a^2 + b^2)^{-\frac{1}{2}} \text{ and } y_v = 0. \quad (3.36)$$

In this case  $f$  has a singularity of the form

$$(z - z_0)^{-\frac{1}{2}} , \quad (3.37)$$

at the point

$$z_0 = 2b^2(a^2 + b^2)^{-\frac{1}{2}} , \quad (3.38)$$

i.e. at the focus F of H.

#### 4. Numerical Examples.

In this section we present several examples illustrating the practical significance of the results of Sections 2 and 3, in connection with numerical conformal mapping techniques. Each example concerns the numerical conformal mapping of a simply-connected domain  $\Omega$ , where the approximation to the mapping function  $f$  is computed by using the so-called Bergman kernel method (BKM). This is an expansion method based on the theory of the Bergman kernel function  $K(z, 0)$  of  $\Omega$ .

Let  $L_2(\Omega)$  be the Hilbert space of all square integrable analytic function in  $\Omega$ . Then the kernel  $K(z, 0)$  has the reproducing property

$$h(0) = \iint_{\Omega} h(z) \overline{K(z, 0)} \, dx dy, \quad \forall h \in L_2(\Omega), \quad (4.1)$$

and is related to the mapping function  $f$  by means of

$$f'(z) = \left\{ \frac{\pi}{K(0, 0)} \right\}^{\frac{1}{2}} K(z, 0); \quad (4.2)$$

see e.g. Bergman [1], Gaier [3] and Nehari [6].

In the BKM the approximation to  $f$  is obtained from (4.2) after first approximating the kernel  $K(z, 0)$  by a finite Fourier series sum. More specifically, if  $\{\eta_j(z)\}$  is a complete set of  $L_2(\Omega)$  then the details of the BKM are as follows:

The set  $\{\eta_j(z)\}_{j=1}^n$  is orthonormalized, by means of the Gram-Schmidt process, to give the set of orthonormal functions  $\{\eta_j^*(z)\}_{j=1}^n$ . Then, because of (4.1),

$$K_n(z, 0) = \sum_{j=1}^n \overline{\eta_j^*(0)} \eta_j^*(z), \quad (4.3)$$

is the  $n$ th partial Fourier sum of the kernel function, and hence,



from (4.2)

$$f_n(z) = \left\{ \frac{\pi}{K_n(0,0)} \right\}^{\frac{1}{2}} \int_0^z K_n(\zeta, 0) d\zeta, \quad (4.4)$$

Is the  $n$ th BKM approximation to the mapping function  $f$ .

The significance of the results of Sections 2 and 3 concerns the choice of the basis functions  $\{\eta_j(z)\}$ . A computationally convenient basis is the set of monomials

$$z^{j-1}; \quad j = 1, 2, 3, \dots \quad (4.5)$$

However, the convergence of the resulting polynomial approximations is often extremely slow and, for the reasons explained in [5, Sect. 2] and [7, Sect. 4], the successful application of the BKM requires that the basis set contains terms that reflect the main singular behaviour of  $f$  in  $\text{compl}(\Omega)$ . This can be achieved by using an "augmented basis", formed by introducing appropriate singular functions into the set (4.5). In particular the augmented basis must contain terms that reflect the singular behaviour of the dominant poles of  $f$ . The purpose of the examples considered below is to illustrate the importance of introducing such terms into the basis set.

If  $\Omega$  involves sharp corners then the augmented basis must also contain terms that reflect the singular behaviour of  $f$  in each of these corners. The problem of choosing appropriate singular functions for dealing with corner singularities is discussed fully in [5] and [7], and is not considered further in the present paper. For this reason, in each of the examples considered below, the domain is constructed so that any two consecutive analytic arcs of its boundary intersect at right angles. In this way the resulting corner singularities are not

serious and can be ignored; see [5, Sect. 2.2] and L7, Sect. 4.2].

The computational details of the BKM procedure used in the examples are exactly as described in [5, Sect. 3] and [7, Sect. 5]. In particular, the estimate  $E_n$  of the maximum error in  $|f_n(z)|$  is obtained, as in [5] and [7], by computing

$$e_n(z) = 1 - |f_n(z)|, \quad (4.6)$$

at a number of "boundary test points"  $z_j \in \partial\Omega$ , and then determining

$$E_n = \max_j |e_n(z_j)|. \quad (4.7)$$

Also, in each example, the numerical results presented correspond to the approximation  $f_{N_{opt}}$ , where  $n = N_{opt}$  is the 'optimum number' of basis functions which gives maximum accuracy in the sense described in [5, p.177] and [7, p.295]. That is, this number is determined by computing a sequence of approximations  $\{f_n(z)\}$ , where at each stage the number  $n$  of basis functions is increased by one. If at the  $(n+1)$ th stage the inequality

$$E_{n+1} < E_n \quad (4.8)$$

is satisfied then the approximation  $f_{n+2}$  is computed. When for a certain value of  $n$ , due to numerical instability, (4.8) no longer holds then we terminate the process and take  $n = N_{opt}$ .

In presenting the results we adopt the notation used in [5] and [7], and denote the BKM with monomial basis (4.5) by BKM/MB and the BKM with augmented basis by BKM/AB.

Example 4.1.

Let  $\Omega_b$ , be the domain bounded by the elliptical arc  $\widehat{DAB} = \{z: z = 5(-e/2 + \cos s) + ib \sin s, -\pi/2 < s < \pi/2\}$ ,  $0 < b < 5$ , and the straight line

$$\overline{BCD} = \{z: z = x + iy, x = -5e/2, -b < y < b\},$$

where

$$e = (25 - b^2)^{\frac{1}{2}}/5$$

is the eccentricity of the ellipse; see Fig. 4.1.

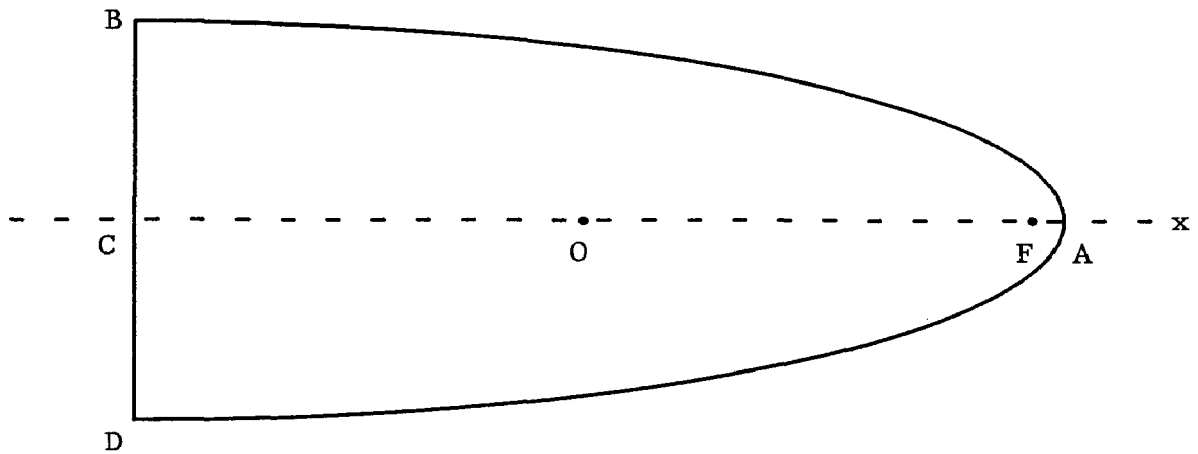


Figure 4.1.

Since the origin 0 lies halfway between the centre C and the focus F of the ellipse, the situation regarding the poles of the mapping function  $f$  with respect to arc  $\widehat{DAB}$  is as described in 3.1.2(a). That is,  $f$  has simple poles at the points  $z_1, z_2$  where, from (3.9),

$$z_1 = \{b^2 + i5\sqrt{3}b\}/(25 - b^2)^{\frac{1}{2}} \quad \text{and} \quad z_2 = \bar{z}_1.$$

The function  $f$  also has a simple pole with respect to the straight line  $\overline{BCD}$  at the point

$$z_3 = -(25 - b^2)^{\frac{1}{2}},$$

the mirror image of 0 in  $\overline{BCD}$ . Thus the augmented basis set, used in the BKM/AB for approximating the kernel

$$K(z,0) = \left\{ \frac{K(0,0)}{\pi} \right\}^{\frac{1}{2}} f'(z),$$

is

$$\eta_j(z) = \left\{ \frac{z}{z - z_j} \right\}^j; \quad j = 1, 2, 3, \quad \eta_{j+3} = z^{j-1}; \quad j = 1, 2, 3, \dots$$

The numerical results obtained for various values of  $b$  are listed in Table 4.1.

Table 4.1

b	BKM/MB		BKM/AB	
	N <sub>opt</sub>	E <sub>N<sub>opt</sub></sub>	N <sub>opt</sub>	E <sub>N<sub>opt</sub></sub>
3	43	1.5 x 10 <sup>-8</sup>	11	4.8 x 10 <sup>-11</sup>
2	30	2.9 x 10 <sup>-8</sup>	15	1.3 x 10 <sup>-10</sup>
1	24	7.9 x 10 <sup>-4</sup>	16	4.8 x 10 <sup>-9</sup>
1/2	22	3.6 x 10 <sup>-2</sup>	20	2.5 x 10 <sup>-7</sup>
1/3	20	1.1 x 10 <sup>-1</sup>	19	3.4 x 10 <sup>-5</sup>
1/4	21	1.7 x 10 <sup>-1</sup>	19	2.2 x 10 <sup>-4</sup>
1/5	19	2.3 x 10 <sup>-1</sup>	21	5.0 x 10 <sup>-4</sup>

#### Example 4.2.

The purpose of this example is to illustrate the critical effect that the position of the origin has on the quality of the approximation. In order to do this we consider the domain  $\Omega_b$  Ex. 4.1 translated

by an amount  $5e/2$  in the negative  $x$ -direction so that

$$\widehat{DAB} = \{z : z = 5(-e + \cos s) + ib \sin s, -\pi/2 < s < \pi/2\}$$

and

$$\overline{BCD} = \{z : z = x + iy, x = -5e, -b < y < b\}.$$

In this way the origin  $0$  coincides with the focus  $F$  and, from R3.1.2(c), the mapping function  $f$  has a double pole with respect to arc  $\widehat{DAB}$  at the point

$$z_1 = 2b^2(25 - b^2)^{-\frac{1}{2}}.$$

As in Ex. 4.1,  $f$  also has a simple pole at the mirror image of  $0$  with respect to  $\overline{BCD}$ , i.e. at the point

$$z_2 = -2(25 - b^2)^{\frac{1}{2}}.$$

Thus, in this case, the augmented basis used in the BKM/AB is

$$\eta_1(z) = \left\{ \frac{z}{(z - z_1)^2} \right\}', \quad \eta_2(z) = \left\{ \frac{z}{z - z_2} \right\}', \quad \eta_{j+2}(z) = z^{j-1}; \quad j = 1, 2, 3, \dots$$

Table 4.2.

b	BKM/MB		BKM/AB	
	Nopt	$E_{\text{Nopt}}$	Nopt	$E_{\text{Nopt}}$
3	14	$2.8 \times 10^{-4}$	15	$2.3 \times 10^{-7}$
2	13	$2.2 \times 10^{-2}$	14	$8.3 \times 10^{-5}$
1	11	$2.7 \times 10^{-1}$	13	$3.3 \times 10^{-3}$

The numerical results obtained, for the three cases where  $b = 3, 2, 1$ , are listed in Table 4.2. These results, like those of Table 4.1, illustrate the improvement in accuracy achieved by

introducing into the basis set functions that reflect the singular behaviour of the dominant poles of  $f$ . However, both the BKM/MB and BKM/AB approximations to the present  $f$  are considerably less accurate than the corresponding approximations to the mapping function of Ex. 4.1. The reason for this is that in the present example the origin  $0$  lies close to the boundary of  $\Omega$ . The difficulty is due entirely to the position of  $0$ , and can be overcome quite simply by observing that  $f$  is connected to the mapping function  $f_1$  of Ex. 4.1 by means of

$$f(z) = \frac{|\alpha|}{\alpha} \left\{ \frac{f_1(z) - \alpha}{1 - \bar{\alpha} f_1(z)} \right\}, \quad \alpha = f_1(ae/2). \quad (4.9)$$

If the BKM/AB approximations to  $f_1$  are used in (4.9) then the resulting approximations to  $f$  are of comparable accuracy to the BKM/AB approximations of Ex. 4.1.

### Example 4.3.

Let  $\Omega$  be the domain bounded by the elliptical arc  $\widehat{LMN}$ , the straight lines  $\overline{NP}$  and  $\overline{LR}$  and the circular arc  $\widehat{PQR}$ , illustrated in Figure 4.2. The details of Figure 4.2 are as follows:

$$\widehat{LMN} = \{z: z = (-17/2 + 5 \cos s) + 3i \sin s, -\pi/5 < s < \pi/5\},$$

$K$  is the point where the normals to the ellipse at  $L$  and  $N$  cut the  $x$ -axis,  $\overline{NP}$  and  $\overline{LR}$  are segments of these normals and  $\widehat{PQR}$  is an arc of the circle with centre at the point  $K$  and radius  $KQ$ , where  $Q = (7/2, 0)$ .

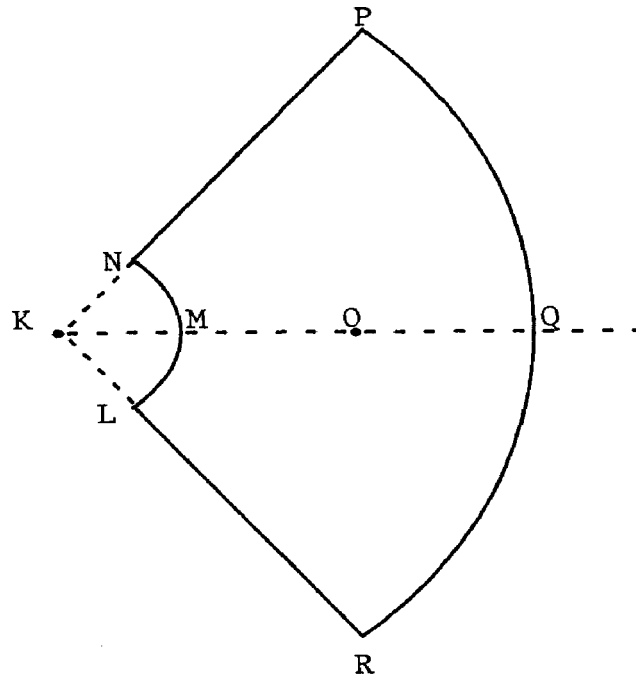


Figure 4.2

The co-ordinates  $x_c = -17/2$ ,  $y_c = 0$  of the centre of the ellipse satisfy (3.11), i.e. the origin  $0$  and the focus  $F = (-9/2, 0)$  are inverse points with respect to arc  $\overline{LMN}$ . Therefore, from R.3.1.2', the mapping function  $f$  has a singularity of the form

$$(z + 9/2)^{-\frac{1}{2}}$$

at  $F$ . The function,  $f$  also has simple poles at the mirror images  $z_1, z_2$  of  $0$  with respect to  $\overline{NP}$  and  $\overline{LR}$ , and at the geometric inverse  $z_3$  of  $0$  with respect to arc  $\overline{PQR}$ . Thus, the augmented basis used in the BKM/AB is

$$\eta_j(z) = \left\{ \frac{z}{z - z_j} \right\}', \quad j=1,2,3, \quad \eta_4(z) = \left\{ \frac{z}{(z + 9/2)^{\frac{1}{2}}} \right\}',$$

$$\eta_{j+4}(z) = z^{j-1}, \quad j=1,2,3,\dots,$$

where in  $\eta_4$  the branch cut of the square root is taken along the line  $x < -9/2$ ,  $y = 0$ .

The numerical results obtained are as follows;

$$\text{BKM/MB: } N_{\text{opt}} = 35, \quad E_{35} = 1.8 \times 10^{-2}$$

$$\text{BKM/AB: } N_{\text{opt}} = 23, \quad E_{23} = 4.4 \times 10^{-5}$$

Example 4.4.

Let  $\Omega_\alpha$  be the domain bounded by the two parabolic arcs

$$\widehat{ABC} = \{z: z = (-0.4 - 0.6a^2 + s^2) - 2is, -\alpha < s < \alpha\}, \alpha > 1,$$

and

$$\widehat{CDA} = \{z: z = (0.6 + 0.4a^2 - s^2) + 2i\alpha s, -1 < s < 1\},$$

which intersect orthogonally at the points A and C; see Figure 4.3.

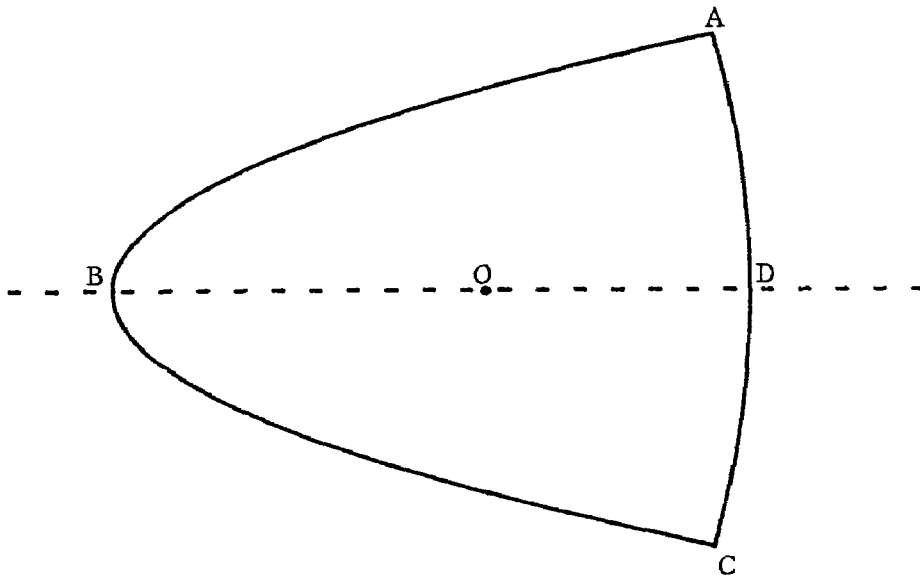


Figure 4.3.

Because of the position of the origin, the poles of the mapping function  $f$  with respect to the arcs  $\widehat{ABC}$  and  $\widehat{CDA}$  are as described in R3.2.2(a) and R3.2.1 respectively. That is,  $f$  has two simple poles



with respect to arc  $\widehat{ABC}$  at the points

$$z_1 = -4 + 4i(0.6\alpha^2 - 0.6)^{\frac{1}{2}} \text{ and } z_2 = \bar{z}_1,$$

and a simple pole with respect to arc  $\widehat{CDA}$  at the point

$$z_3 = 4\alpha \{ \alpha - (0.6\alpha^2 - 0.6)^{\frac{1}{2}} \}. \text{ Thus the augmented basis used}$$

in the BKM/AB is

$$\eta_j(z) = \left\{ \frac{z}{z - z_j} \right\}'; \quad j = 1, 2, 3, \quad \eta_{j+3}(z) = z^{j-1}; \quad j = 1, 2, 3, \dots$$

The numerical results obtained, for the three cases where  $\alpha = 2, 5, 10$ , are listed in Table 4.3.

Table 4.3

$\alpha$	BKM/MB		BKM/AB	
	N <sub>opt</sub>	E <sub>N<sub>opt</sub></sub>	N <sub>opt</sub>	E <sub>N<sub>opt</sub></sub>
2	32	$5.8 \times 10^{-9}$	13	$1.8 \times 10^{-10}$
5	36	$1.6 \times 10^{-7}$	16	$2.4 \times 10^{-10}$
10	24	$2.2 \times 10^{-3}$	18	$1.5 \times 10^{-8}$

Example 4.5

Let  $\Omega$  be the domain bounded by the two hyperbolic arcs

$$\widehat{ABC} = \{z: z = (-x_0 + 2 \cosh s) + i(-y_0 + \sinh s), \quad s_1 < s < s_2\},$$

and

$$\widehat{CDA} = \{z: z = (x_0 - 2 \cosh s) + i(y_0 - \sinh s), \quad s_1 < s < s_2\},$$

where

$$X_0 = \cosh s_1 + \cosh s_2, \quad y_0 = (\sinh s_1 + \sinh s_2)/2$$

are the co-ordinates of the centre of arc  $\widehat{CDA}$ . We take  $s_2 = 1$  and choose  $s_1$ , so that

$$4 \tanh s_1 \tanh s_2 + 1 = 0.$$

In this way the two arcs intersect orthogonally at A and C; see Figure 4.4.

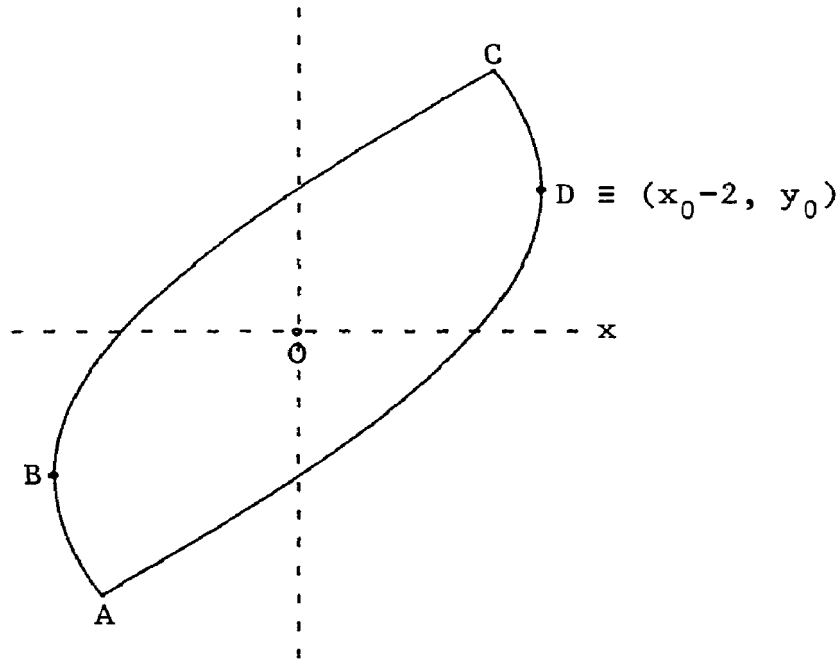


Figure 4.4

Because of the position of the origin the poles of the mapping function  $f$  with respect to both arc  $\widehat{ABC}$  and arc  $\widehat{CDA}$  are as described in R3.3.1. That is, from (3.33),  $f$  has simple poles at the points

$$z_1 = z_0 - \{3\bar{z}_0 + 4i(\bar{z}_0^2 - 5)^{\frac{1}{2}}\}/5 \quad \text{and} \quad z_2 = -z_1,$$

where  $z_0 = x_0 + iy_0$ . The symmetry of the domain implies that the polynomial representation of the kernel function involves only even powers of  $z$ , and that the augmented basis may be taken to be

$$\eta_1(z) = \left\{ \frac{2z_1 z}{z^2 - z_1^2} \right\}', \quad \eta_{j+1}(z) = z^{2(j-1)}; \quad j = 1, 2, 3, \dots$$

The numerical results obtained are as follows:

$$\text{BKM/MB: } N_{\text{opt}} = 13, \quad E_{13} = 1.5 \times 10^{-4}.$$

$$\text{BKM/AB: } N_{\text{opt}} = 12, \quad E_{12} = 3.1 \times 10^{-8}.$$

Example 4.6.

Let  $\Omega$  be the domain bounded by the straight lines

$$\overline{AB} = \{z: z = x + iy, -2 < x < 2, y = -1/3\},$$

$$\overline{BC} = \{z: z = x + iy, x = 2, -1/3 < y < 1\},$$

$$\overline{EA} = \{z: z = x + iy, x = -2, -1/3 < y < 1/3\},$$

and the arc

$$\widehat{EDC} = \{z: z = c(s), -2 < s < 2\},$$

where

$$c(s) = s + i\{2/3 + s/4 - s^3/48\};$$

see Figure 4.5. In the figure, the point D has x-coordinate

$$x_D = -0.156,$$

and is chosen so that the line  $\overline{OD}$  is nearly normal to arc  $\widehat{EDC}$ .

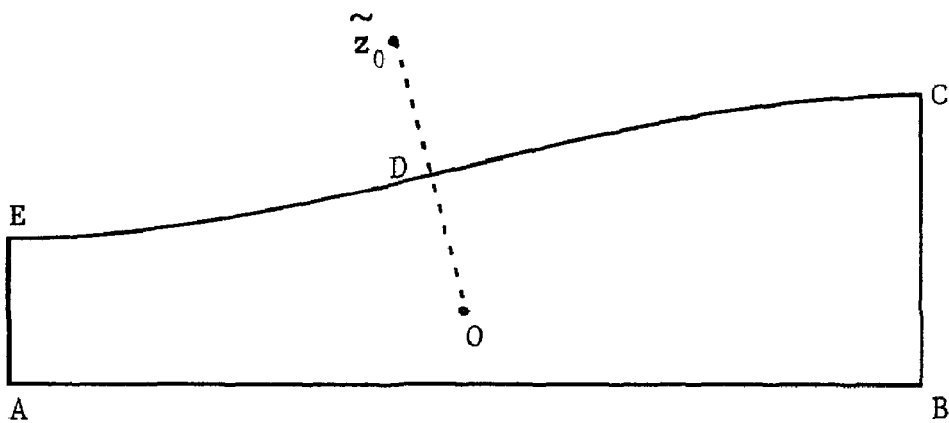


Figure 4.5

A BKM approximation to the mapping function  $f$  is given in [8, Ex. 2.2]. This approximation is computed by using an augmented basis obtained by introducing into the monomial set (4.5) the functions

$$\left\{ \frac{z}{z-z_j} \right\}; \quad j=1,2,3, \quad (4.10)$$

and

$$\left\{ \frac{z}{z-\tilde{z}_0} \right\}, \quad (4.11)$$

where

$$z_1 = -2i/3, \quad z_2 = 4, \quad z_3 = -4,$$

are the mirror images of 0 with respect to  $\overline{AB}$ ,  $\overline{BC}$  and  $\overline{EA}$ , and

$$\begin{aligned} \tilde{z}_0 &= 2z_D \\ &= -0.312 + i 1.2555 491 517 33. \end{aligned}$$

Thus, the basis set used in [8] contains the three singular functions (4.10) which correspond to the simple poles that  $f$  has with respect to the straight lines  $\overline{AB}$ ,  $\overline{BC}$  and  $\overline{EA}$ ,. However, the choice of the singular function (4.11) is based entirely on intuitive arguments, which suggest that  $f$  might have a simple pole with respect to arc  $\widehat{EDC}$  at some point near the point  $\tilde{z}_0$ . The precise nature of the poles of  $f$  with respect to arc  $EDC$  can be determined, by means of the technique of Section 2, as follows.

By using the Newton-Raphson method we find that the equation

$$c(\zeta) = 0$$

has a root at the point

$$\zeta_0 = -0.159 775 271 90 -i 0.622 932 820 27$$

and that

$$\begin{aligned} z_0 &= c(\bar{\zeta}_0) \\ &= -0.319\ 550\ 543\ 81 + i\ 1.245\ 865\ 640\ 54. \end{aligned}$$

Also, it can be shown easily that

$$c(\zeta_1) - c(\zeta_2) = (\zeta_1 - \zeta_2)R(\zeta_1, \zeta_2),$$

Where

$$R(\zeta_1, \zeta_2) = (1 + i/4) - i(\zeta_1^2 + 2\zeta_1\zeta_2 + \zeta_2^2)/48.$$

Since

$$R(\zeta_1, \zeta_2) \neq 0$$

for all points  $\zeta_1, \zeta_2$  in the rectangle

$$G = \{\zeta: \zeta = s + it, -2 < s < 2, -1 < t < 1\},$$

it follows that the function  $c(\zeta)$  is one-one in  $G$ . Thus, there exists a region  $G^*$  satisfying the conditions C2.1 and C2.2 and containing the points  $\zeta_0$  and  $\bar{\zeta}_0$ . Therefore, by R2.1,  $f$  has a simple pole with respect to arc EDC at  $z_0$ . For this reason, we construct the augmented basis for the BKM/AB by introducing into the monomial set the three functions (4.11) and the function

$$\left\{ \frac{z}{z - z_0} \right\}' \quad (4.12)$$

Our BKM/AB results are listed below and are compared with the results of the BKM/MB and also the results BKM/ $\tilde{AB}$ , obtained in [8] by using the singular function (4.11), instead of (4.12). The numerical results justify completely the choice of the singular function (4.12).

$$\begin{aligned} \text{BKM/MB} & : \text{Nopt} = 23, \quad E_{23} = 5.3 \times 10^{-2} \\ \text{BKM/AB, [8]} & : \text{Nopt} = 22, \quad E_{22} = 4.9 \times 10^{-5} \\ \text{BKM/AB} & : \text{Nopt} = 20, \quad E_{20} = 5.5 \times 10^{-7} \end{aligned}$$

We end this section, by pointing out a difficulty which occurs when the regions  $\Omega_2$  corresponding to two separate analytic arcs of  $\partial\Omega$  overlap. Let  $\Gamma_1$  and  $\Gamma_2$  be two such arcs and denote by  $\Omega_2^{(1)}$  and  $\Omega_2^{(2)}$  the corresponding  $\Omega_2$  regions. Then, in general, the mapping function  $f$  will have two different continuations in  $\Omega_2^{(1)} \cap \Omega_2^{(2)}$  and, for this reason, it might not be possible to reach any conclusions regarding the poles of  $f$  with respect to  $\Gamma_1$  and  $\Gamma_2$ . This situation arises frequently when  $\Gamma_1$  and  $\Gamma_2$  are the arms of a corner, where  $f$  has a branch point singularity which, in general, is much more serious than any poles with respect to  $\Gamma_1$  and  $\Gamma_2$  that our method might predict. Fortunately, the appropriate singular basis functions needed for dealing with branch point singularities can be determined, as in [5] and [7], by considering the asymptotic expansion of  $f$  in a neighbourhood of a corner.

## 5. Discussion

The numerical examples of Section 4 illustrate how the results of Sections 2 and 3, concerning the nature of the "poles" of the mapping function  $f$ , can be used to improve the BKM approximations to  $f$ . Naturally, the accuracy of other expansion methods for numerical conformal mapping can be improved in exactly the same way, by ensuring that the basis set used for approximating  $f$  contains functions that reflect the singular behaviour of the dominant poles of  $f$ .

REFERENCES

- 1 Bergman, S.: The kernel function and conformal mapping.  
Math. Surveys 5, Am. math. Soc., Providence R.I.  
(2nd ed.) 1970.
- 2 Ellacott, S.W.: A technique for approximate conformal mapping.  
Multivariate approximation. (Hadscomb, D., ed.)  
London: Academic Press 1978.
- 3 Gaier, D.: Konstruktive Methoden der konformen Abbildung.  
Berlin-Heidelberg-New York: Springer 1964.
- 4 Henrici, P.: Applied and computational complex analysis, Vol. 1.  
New York: Wiley 1974.
- 5 Levin, D., Papamichael, N., Sideridis, A.: The Bergman kernel  
method for the numerical conformal mapping of simply  
connected domains. J.Inst. Maths. Aplics. 22,  
171-187 (1978).
- 6 Nehari, Z.: Conformal mapping. New York: McGraw-Hill 1952.
- 7 Papamichael, N., Kokkinos, C.A.: Two numerical methods for the  
conformal mapping of simply-connected domains.  
Comput. Meths. Appl. Mech. Engrg, 28. 285-307 (1981).
- 8 Papamichael, N., Sideridis, A.: Formulae for the approximate  
conformal mapping of some simply-connected domains.  
Technical Report TR/72, Dept. of Maths., Brunel University,  
1977.

- 9 Sansone, G., Gerretsen, J.: Lectures on the theory of functions of a complex variable, Vol. II. Groningen: Wolters-Noordhoff 1969.

**NOT TO BE  
REMOVED**  
FROM THE LIBRARY

XB 2356456 3

